

OPEN ACCESS

EDITED BY Jayesh Jagannath Ahire, Dr. Reddy's Laboratories (India), India

REVIEWED BY
Caroll M. Mendonca,
Ginkgo BioWorks (United States),
United States
Xiangfei Li,
Anhui Polytechnic University, China

*CORRESPONDENCE
Gongli Zong

☑ zonggongli@sdfmu.edu.cn
Guangxiang Cao
☑ caoguangxiang@sdfmu.edu.cn

[†]These authors have contributed equally to this work

RECEIVED 12 August 2025 ACCEPTED 10 October 2025 PUBLISHED 27 October 2025

CITATION

Meng Z, Yu M, Wang J, Li H, Gao W, Yang P, Cui X, Zhang P, Fu J, Cao G and Zong G (2025) Abundant organic nitrogen enhances natamycin biosynthesis by increasing NAD(P) metabolic pathway activity in *Streptomyces gilvosporeus* F607.

Front. Microbiol. 16:1684019. doi: 10.3389/fmicb.2025.1684019

COPYRIGHT

© 2025 Meng, Yu, Wang, Li, Gao, Yang, Cui, Zhang, Fu, Cao and Zong. This is an open-access article distributed under the terms of the Creative Commons Attribution License (CC BY). The use, distribution or reproduction in other forums is permitted, provided the original author(s) and the copyright owner(s) are credited and that the original publication in this journal is cited, in accordance with accepted academic practice. No use, distribution or reproduction is permitted which does not comply with these terms.

Abundant organic nitrogen enhances natamycin biosynthesis by increasing NAD(P) metabolic pathway activity in *Streptomyces gilvosporeus* F607

Zhihui Meng^{1†}, Minghui Yu^{1†}, Jiahui Wang¹, Haijun Li², Wenhui Gao¹, Peitong Yang¹, Xingyu Cui¹, Peipei Zhang¹, Jiafang Fu¹, Guangxiang Cao^{1*} and Gongli Zong^{1*}

¹Biomedical Sciences College and Shandong Medicinal Biotechnology Centre, Key Lab for Genetic Engineering and Synthetic Biology of Shandong Province, Shandong First Medical University and Shandong Academy of Medical Sciences, Ji'nan, China, ²Shandong Freda Biotechnology Co., Ltd., Linyi, China

Natamycin, a polyene macrolide antifungal produced by several Streptomyces species, is widely used as an industrial mold inhibitor in food preservation. Although nitrogen source effects on its production have been extensively studied, its underlying regulatory mechanisms remain unclear. Using transcriptome and metabolome analyses, we found that natamycin production increase by 2.8-fold during cultivation of Streptomyces gilvosporeus F607 in organic nitrogen-rich medium, accompanied by upregulation of 10 genes involved in NAD(P) biosynthesis and corresponding elevations in the levels of NAD or NADP with 1.81-fold and 1.04-fold increases. A novel multisubstrate enzyme, designated nicotinic acid mononucleotide (NaMN) adenylyltransferase (NadDsg), was demonstrated to slightly favor nicotinamide mononucleotide (NMN) over NaMN. Supplementation of S. gilvosporeus F607 with 10 mg/L NMN and overexpression of a site-directed mutant enzyme (NadDsg $_{\mbox{\scriptsize RYKK}}$, at positions of $R^{17}Y^{20}K^{26}R^{168}$) promoted natamycin biosynthesis by 43.1%, increasing production from 4.67 g/L to 6.68 g/L. These findings indicate that an abundance of organic nitrogen primarily enhances natamycin biosynthesis by elevating NAD(P) levels, providing valuable insights for medium optimization and strain engineering toward high-yield natamycin production.

KEYWORDS

natamycin biosynthesis, NAD (P) metabolism, NMN, NadD, metabolic engineering

1 Introduction

Nitrogen sources, ranging from simple compounds (e.g., ammonium, nitrate, and nitrite) to complex organic forms, are crucial for primary and secondary metabolism in *Streptomyces* (Krysenko and Wohlleben, 2024). During growth, the diverse nitrogen sources are converted into amino acids and other nitrogen-containing compounds to support the synthesis of cellular building blocks (Fink et al., 2002). Primary metabolism provides nitrogen-containing intermediates or precursors for secondary metabolism (Ryu et al., 2006), which incorporates diverse compounds, such as ammonium, nitrate,

amino acids, amino sugars, and urea (Rodríguez et al., 2018). Antibiotic production in *Streptomyces* is largely affected by the availability of nitrogen sources (Martín and Liras, 2010; Passmore et al., 2021).

Natamycin, a glycosylated 26-membered tetraene macrolide antifungal (Aparicio et al., 2000; Volpon and Lancelin, 2002), is produced by Streptomyces species including S. natalensis (Aparicio et al., 2000), S. gilvosporeus (Liang et al., 2008), S. lydicus (Wu et al., 2013), and S. chattanoogensis (Du et al., 2009). Its antifungal activity is dependent on hydrophobic interactions between the polyene of natamycin and sterols in the fungal cell wall (Antón et al., 2004; Aparicio et al., 2016; Yangla and Yldz, 2016). Natamycin has emerged as a major mold inhibitor in the food industry (Yangla and Yldz, 2016), and shows potential in preventing the proliferation of prostate cancer cells (Vasquez et al., 2020). Optimization of the cultivation medium for natamycin production in S. natalensis has been reported (Farid et al., 2020), and recent findings confirm that nitrogen metabolism plays a crucial role in enhancing its yield (Wang et al., 2025a,b). In S. gilvosporeus strain AG-2, pentose phosphate pathway enhancement, tricarboxylic acid cycle modulation, and overexpression of acetyl-CoA and malonyl-CoA via the nitrogen metabolism regulator glnR were shown to promote natamycin production (Wang et al., 2025b).

Reductive steps in most antibiotic biosynthetic pathways require the co-factor Nicotinamide Adenine Dinucleotide (NAD) Phosphate (NADPH), whose intracellular levels are reportedly influenced by the activities of glucose-6-phosphate dehydrogenase and 6-phosphogluconate dehydrogenase in the pentose phosphate pathway (PPP) (Butler et al., 2002). Natamycin, like other macrocyclic polyketides, is synthesized by type I modular Polyketide Synthases (PKSs), which sequentially assemble carbon chains from small acyl precursors (Aparicio et al., 2003). During synthesis of the polyketide macrolactone backbone, the ketosynthase domain of PKS catalyzes ketoreduction using the 4pro-S hydride of NADPH, yielding a β-hydroxy thioester product (Passmore et al., 2021). Thus, biosynthesis of polyene macrolide polyketides requires adequate NADPH as a co-factor providing reducing power (Borgos et al., 2006; Zhang et al., 2020). Enhanced nitrogen metabolism has been proposed to indirectly increase NADPH reducing power by upregulating glycolysis and the PPP pathway (Wang et al., 2025b). However, the mechanism by which organic nitrogen sources affect natamycin biosynthesis remains unclear.

In this study, we investigated the effects of organic nitrogen on natamycin biosynthesis in *S. gilvosporeus* strain F607 through transcriptome and metabolome analyses. We found that increased biosynthesis of NAD (P), originating from the aspartate (Asp) oxidase and quinolinate (QA) synthesis pathways, enhanced reducing power during natamycin biosynthesis. Furthermore, modification of nicotinic acid mononucleotide adenylyltransferase (NadD), the rate-limiting enzyme in the NAD (P) synthesis pathway, reduced the accumulation of Nicotinic Acid (NA) and improved both NAD(P) levels and natamycin yield. Our findings reveal specific alterations in the NAD (P) synthesis pathway in *S. gilvosporeus* and provide insights into medium optimization and fermentation design for improving natamycin production.

2 Methods

2.1 Strains and cultures

S. gilvosporeus strain F607 (GenBank accession no. CP020569) was cultured in seed medium containing 10 g/L glucose, 5 g/L peptone, 3 g/L yeast extract, and 3 g/L malt extract for 24 h. To induce fermentation for natamycin production, 5% of the seed culture was used to inoculate low-nitrogen NTL medium (2.0 g/L soy peptone, 0.45 g/L yeast extract, 2.0 g/L NaCl, 1.0 g/L MgSO₄, 60.0 g/L glucose, pH 7.5) or high-nitrogen NTH medium (20 g/L soy peptone, 4.5 g/L yeast extract, 2.0 g/L NaCl, 1.0 g/L MgSO₄, 60.0 g/L glucose, pH 7.5). The strains used are listed in Supplementary Table 1.

2.2 Ultra-High Performance Liquid Chromatography (UHPLC) coupled with Q Exactive (QE) Mass Spectrometry (MS) detection of intracellular metabolites

A 4-mL bacterial culture grown in NTH fermentation broth was centrifuged at 10,000 rpm to collect the cells, which were then washed thrice with phosphate-buffered saline solution. 1,000 μL extract solution (methanol: acetonitrile: water = 2: 2: 1, with isotopically-labeled internal standard mixture) was added into 20 mg sample. Then the samples were homogenized at 35 Hz for 4 min and sonicated for 5 min in ice-water bath. The homogenization and sonication cycle were repeated for 3 times. Then the samples were incubated for 1 h at -40° C and centrifuged at 12,000 rpm for 15 min at 4°C. The resulting supernatant was transferred to a fresh glass vial for analysis. The quality control (QC) sample was prepared by mixing an equal aliquot of the supernatants from all of the samples. UHPLC-QE-MS detection of intracellular metabolites was performed by Biotree Biomedical Technology Co., Ltd. (Shanghai, China), using a Vanquish UHPLC system (Thermo Fisher Scientific, MA, USA) with a UPLC ethylene-bridged hybrid (BEH) amide column (2.1 \times 100 mm, 1.7 μ m) coupled to an Orbitrap QE HFX mass spectrometer (Thermo Fisher Scientific). Mobile phase A (25 mmol/L ammonium acetate and 25 mmol/L ammonia hydroxide in water [pH 9.75]) and mobile phase B (100% acetonitrile) were used for both positive and negative modes of electrospray ionization (ESI). The ESI source conditions were as follows: sheath gas flow rate, 30 Arb; auxiliary gas flow rate, 25 Arb; capillary temperature, 350° C; full MS resolution, 60,000; tandem MS/MS resolution, 7,500; collision energy, 10/30/60 in normalized collision energy mode; and spray voltage, 3.6 kV (positive) or 23.2 kV (negative). The raw data were converted to the mzXML format using ProteoWizard and processed with an in-house program, which was developed using R and based on XCMS, for peak detection, extraction, alignment, and integration. Then an in-house MS2 database (BiotreeDB) was applied in metabolite annotation. The cutoff for annotation was set at 0.3.

2.3 Transcriptomic analyses

For transcriptome sequencing and analysis, F607 mycelia were harvested after 24, 60, and 120 h of culture in different media. 1 mL fermentation culture was centrifuged at 5,000 rpm at 4 °C for 5 mins for twice and resuspend by TE buffer. Bacterial suspension was grinded in a clean, liquid nitrogen cooled mortar. Add liquid nitrogen once every 1 min, and grind 2-3 times. RNA was extracted by using the RNA Extraction Kit (Baiteke, Beijing). RNA integrity was assessed using the Bioanalyzer 2,100 system (AgilentTechnologies, CA, USA). The transcriptomes were sequenced using an Illumina HiSeq 3000 sequencer at Novogene Corporation (Tianjin, China). HTSeq v0.6.1 was used to count the reads numbers mapped to each gene. And then FPKM of each gene was calculated based on the length of the gene and reads count mapped to this gene. FPKM, expected number of Fragments Per Kilobase of transcript sequence per Millions base pairs sequenced, considers the effect of sequencing depth and gene length for the reads count at the same time, and is currently the most used method for estimating gene expression levels. The resulting *P*-value is adjusted using the Benjamini and Hochberg methods to control the error discovery rate. The corrected *P*-value < 0.05 was set as the threshold of significant differential expression.

2.4 Molecular simulation analyses

Protein sequences were aligned using CLUSTALW2 (http://www.expasy.ch). Sequences were retrieved using the protein search algorithm at the National Center for Biotechnology Information (NCBI), and conserved NadD domains were identified via NCBI's CD-Search. Multiple sequence comparison was carried out using Clustal Omega (Madeira et al., 2019) and ESPript software (Xavier and Patrice, 2014). A homology model of NadD was constructed using Robetta (https://robetta.bakerlab.org/) and Discovery Studio 2.0 (BIOVIA., 2017). Molecular docking analyses of nicotinic acid mononucleotide (NaMN) and NA were performed using the CDOCKER protocol of Discovery Studio 2.0 (BIOVIA., 2017).

2.5 Computer-assisted directed evolution of NadD

Virtual saturation mutagenesis of NadD was performed using MaxFlow (https://maxflow.ilabpower.com). To identify variants with increased affinity for nicotinamide mononucleotide (NMN) and reduced affinity for NaMN, 17 residues Met15, Gly16, Gly17, Thr18, Phe19, His26, Thr113, Gly114, Ser168, Asp20, Pro21, Ile112, Tyr92, Thr93, Ile94, Trp124, and His125 were individually mutated, and their interactions with NMN were evaluated. Virtual variants with predicted improvement of NMN binding ability (ΔG total (kcal/mol) < 0) were selected as candidates for the next evaluation. Next, the mutational nadD gene was cloned into the pET15-b vector, which carries an N-terminal His-tag. Sitedirected metagenesis was performed by incubating template DNA, dNTPs, and the appropriate mutagenic primers with Pfu DNA polymerase, in accordance with the manufacturer's instruction

manual. Mutant plasmids were verified by DNA sequencing and transformed into *Escherichia coli* BL21 (DE3) for recombinant protein expression and purification. Intracellular concentrations of NAD⁺ were determined as previously described (Zhang et al., 2009).

2.6 Expression and purification of wild-type and variant NadDsg

The *nadDsg* gene, a *nadD* homolog, was amplified from *S. gilvosporeus* F607 genomic DNA using the primer pair *nadDsg* His-F/R (Supplementary Table 1) and then cloned into pMD18T to generate pMD18T-nadDsg. After confirmation by DNA sequencing, *nadDsg* from pMD18T-nadDsg was cloned into the expression vector pET-15b to construct pET-nadDsg, which was transformed into *E. coli* BL21 (DE3) to obtain *E. coli* BL21/pET-nadDsg. BL21/pET-nadDsg was cultured to an OD_{600nm} of 0.6–0.8, and NadDsg expression was induced by the addition of 0.1 mM isopropyl-D-1-thiogalactopyranoside. His₆-NadDsg fusion proteins were purified by Ni-NTA chromatography (Sangon Biotech, Shanghai, China) (Fu et al., 2019). The *nadDsg* mutants were cloned and synthesized by Sangon Biotech, and the variant proteins expressed and purified using the same protocol.

2.7 Detection of enzymatic reactions in vitro

For enzymatic quantification, levels of NAMN, NMN, ATP, nicotinic acid adenine dinucleotide (NAAD), and NAD were measured using HPLC, as previously reported (Mehl et al., 2000). Briefly, the substrates and enzyme in reaction buffer (100 mM Tris-HCl, 2.0 mM MgCl₂, pH 8.0) were incubated with 2 mM ATP at 37° C for the appropriate time interval, and 20-mL aliquots were analyzed by high-pressure liquid chromatography (HPLC). HPLC was performed on Agilent Series 1,200 system (Agilent Technologies, CA, USA) with a diode array ultraviolet detector set at 254 nm and a Zorbax Eclipse XDB-C18 column. Buffer A contained 100 mM KH₂PO₄ (aqueous), pH 7.5. Buffer B contained 80% 100 mM KH₂PO4 (aqueous), pH 7.5, and 20% methanol. Elution conditions were as follows: 100% buffer A for 0 to 7 min; 100% buffer A to 100% buffer B in 7 to 8 min; and 100% buffer B for 8 to 13 min. The flow rate was 1 mL/min.

2.8 Construction of *nadD* mutant strains and effect on natamycin production

An additional *nadD* mutant strain was constructed via *att* integration, as previously described (Gongli et al., 2022). Briefly, nadD mutant genes were cloned downstream of the ermE promoter region in the integrative vector pSET152 (Sangon Biotech, Shanghai, China) to generate pSET152-nadD_M, which was then introduced into the genome of *S. gilvosporeus* F607 via intergeneric conjugation using *E. coli* ET12567 as the donor strain. Nalidixic acid (500 μ g) and apramycin (1 mg) were added, and the culture

was incubated for a further 5 days to select the exconjugants. Successful conjugants were confirmed by colony PCR using primers nadD V-F1 and nadD V-R1, and by DNA sequencing. Wild type *nadDsg* was used as a control. Natamycin was quantified by HPLC analysis, as previously described (Wang et al., 2016).

3 Results

3.1 Organic nitrogen availability influences nicotinate/nicotinamide metabolism and natamycin production

Nitrogen metabolism plays crucial roles in promoting natamycin production (Wang et al., 2025a). To investigate the impact of organic nitrogen content on natamycin biosynthesis, we cultured *S. gilvosporeus* F607 in two media formulations: NTH fermentation medium (20 g/L soy peptone and 4.5 g/L yeast extract) and NTL medium (2.0 g/L soy peptone and 0.45 g/L yeast extract). In NTL medium, containing low organic nitrogen, the maximum production of natamycin was 20.35 mg/g mycelium. In contrast, natamycin increased by 2.8-fold (reaching to 77.38 mg/g mycelium) when F607 was cultivated in NTH medium resulted (Figure 1A).

Metabolome analysis comparing intracellular profiles of F607 cultured in NTH and NTL media across the early (24 h), rapid (60 h), and later (120 h) stages of natamycin biosynthesis, revealed differential activity in nitrogen metabolism and several amino acid metabolism pathways, including arginine/proline, D-Glutamine/glutamate, beta-alanine, D-alanine histidine, and alanine/aspartate. Notably, metabolism of nicotinate and nicotinamide was identified across all three stages of natamycin biosynthesis and ranked among the top 10 pathways (Figures 1B–D).

Next, changes in three important metabolites in the nicotinate and nicotinamide metabolic pathway—NAMN, NAM (Niacinamide), and NA—were analyzed. At the early stage of natamycin biosynthesis, NAMN levels decreased (22.0%, p < 0.01), while NA was enriched (284.1%, p < 0.01) in the NTH cultivation group compared with that in the NTL group (Figure 1E). At the later stage, levels of both NAM and NAMN decreased (26.82% and 2.16%, respectively, p < 0.01) in the NTH group (Figure 1E). At the rapid stage, levels of NAMN and NAM were significantly lower (10.03% and 36.88%, p < 0.01) in the NTH group than in the NTL group (Figure 1E), indicating higher consumption of these precursors during high-yield natamycin biosynthesis.

NAM, NA, and NAMN are key intermediates in the biosynthesis of NADH and NADPH. Considering the demand for reducing power during natamycin biosynthesis, we quantified total NAD+/NADH and NADP+/NADPH concentrations at the rapid stage. Total NAD+/NADH (1.77 μ g/g dry cell weight [DCW]) and total NADP+/NADPH (0.94 μ g/g DCW) concentrations in the NTH cultivation group were higher than those in the NTL group (0.63 μ g/g DCW and 0.46 μ g/g DCW, respectively), representing 1.81-fold and 1.04-fold increases (Figure 1F). These findings indicated a directed metabolic flow from NAM and NAMN to NAD (H) and NADP(H) biosynthesis during rapid natamycin production under conditions of abundant organic nitrogen.

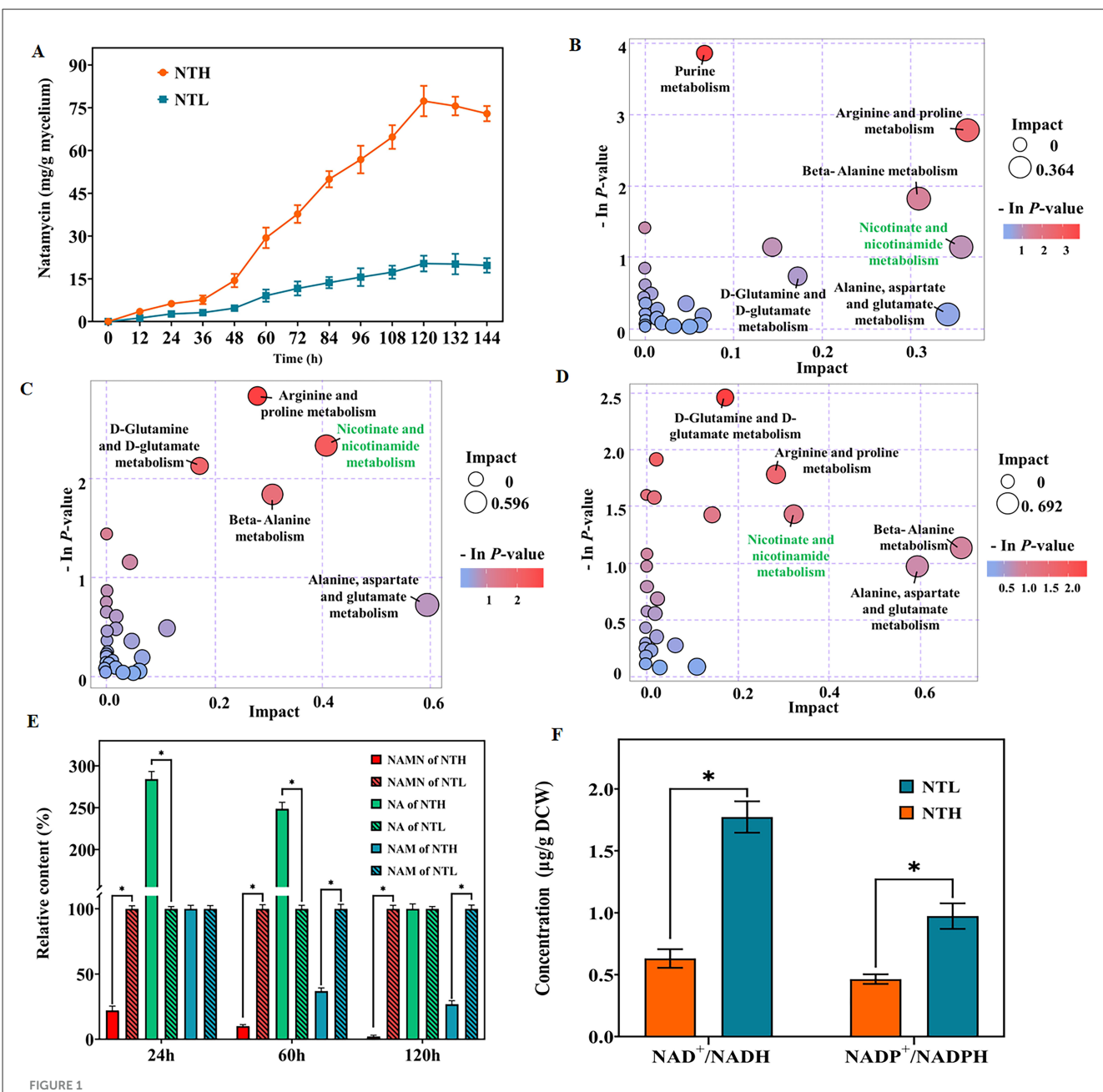
3.2 Abundant organic nitrogen affects genetic expression of the NAD+/NADP+ pathway during rapid natamycin biosynthesis

To investigate the mechanism by which organic nitrogen stimulates NAD+/NADP+ and natamycin production in *S. gilvosporeus* F607, we conducted a transcriptome analysis. This revealed upregulation of all genes in the natamycin biosynthetic cluster. Notably, the PKS genes *sgnS4*, *sgnS3*, *sgnS2*, and *sgnS0* exhibited 5.1- to 6.1-fold increases in expression (log₂ fold-change) in the NTH cultivation group compared with that in NTL group during the rapid stage of natamycin biosynthesis (Figure 2 and Supplementary Table 2).

In addition to two *de novo* NAD⁺ biosynthesis pathways (Ding et al., 2021) and a salvage pathway (Wang et al., 2017), a homolog of the Preiss-Handler pathway (Turlo et al., 2012) has also been identified in S. gilvosporeus F607 (Figure 2), based on the genomic sequence (Genebank NO. CP020569). Within the Asp-derived synthesis pathway I illustrated in Figure 2, the NTH group showed upregulation of all eight key genes, including those encoding Asp oxidase (nadB), quinolinate synthase (nadA), QA phosphoribosyl transferase (nadC), NMN/NaMN adenylyltransferase (nadD), and NAD synthase (nadE), compared with the NTL group (Supplementary Table 3), leading to extensive consumption of QA and NAMN. In the Trp-derived pathway II (Figure 2) comprising five key genes, the expression levels of genes encoding tryptophan 2,3-dioxygenase and kynureninase was upregulated while those encoding kynurenine formamidase and kynurenine 3-monooxygenase were downregulated (Supplementary Table 3). Compared with the high expression across all genes in pathway I, the downregulation of two enzymes in pathway II may limit its NAD+ contribution. Therefore, S. gilvosporeus F607 appears to favor pathway I for NAD+ production during the rapid stage of natamycin biosynthesis.

In the Preiss–Handler pathway (Figure 2), expression of the key entry gene *pncB*, which facilitates the incorporation of NA into NAD⁺ biosynthesis, was significantly downregulated, whereas *pncA* was upregulated (Supplementary Table 3). The high expression of *pncA* leads to NAM reduction, while the low expression of *pncB* results in NA accumulation. In the salvage pathway involving NAD⁺ synthesis from NMN (Figure 2), *nadD* was upregulated (Supplementary Table 3). NAD can be synthesized via the amidated pathway, where NMN adenylyltransferase (NMNAT; a NadD homolog) is the key enzyme that directly converts NMN to NAD at the expense of ATP. This route represents an efficient mechanism for NAD⁺ production. However, strain F607 does not carry a gene encoding the nicotinamide phosphoribosyl transferase (NAMPT) enzyme, preventing the direct synthesis of NMN.

In summary, the metabolomic and transcriptomic analyses revealed a link between abundant organic nitrogen, preferential utilization of pathway I for NAD⁺/NADP⁺ synthesis, and rapid natamycin biosynthesis. Increasing NAD⁺ availability through NMN supplementation or modification of the salvage pathway represents a promising strategy for enhancing natamycin biosynthesis.

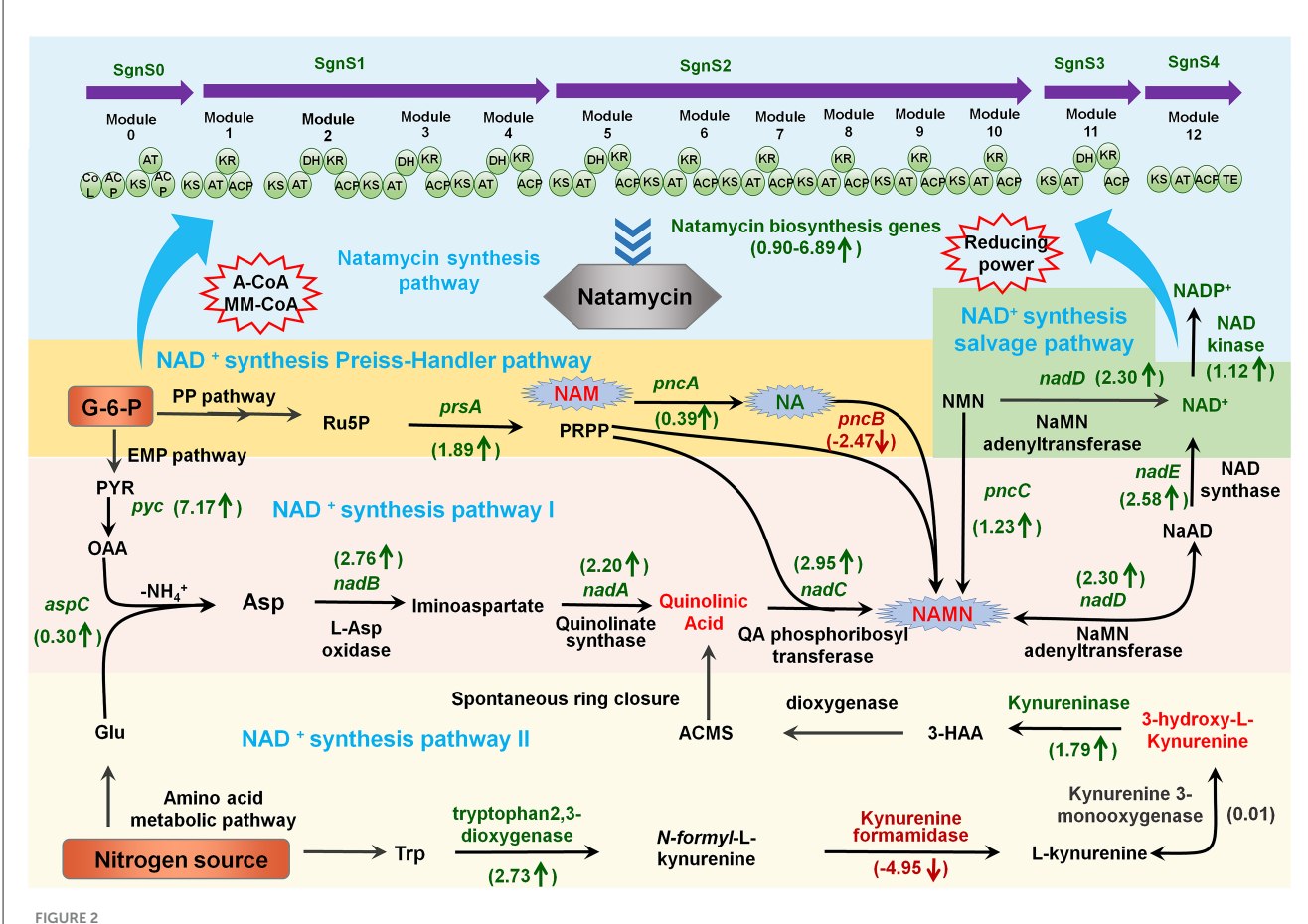


Influence of organic nitrogen availability on natamycin production and nicotinate/nicotinamide metabolism. (A) Natamycin production by S. gilvosporeus cultivated in high-nitrogen (NTH) and low-nitrogen (NTL) media over time. (B–D) Bubble diagrams of pathway analysis of the NTH and NTL groups at the early (24 h; B), rapid (60 h; C), and later (120 h; D) stages of natamycin biosynthesis. (E) Comparison of the levels of key metabolites of the nicotinate/nicotinamide metabolic pathway between the NTH and NTL groups at the three stages. The quantity of each metabolite in NTL group was defined as 100%. (F) Concentrations of total NAD+/NADH and NADP+/NADPH in the two groups at the rapid stage. * p < 0.05.

3.3 NMN supplementation promotes natamycin biosynthesis

Because *S. gilvosporeus* F607 does not carry genes encoding NMN synthesis enzymes (e.g., NAMPT and NMN synthase), it cannot synthesize NMN like most microbes (Xianzhong et al., 2014). However, NMN supplementation of the culture medium is a strategy for enhancing NAD⁺ and natamycin production in the presence of *nadD* in this strain. To further evaluate the impact of NMN on natamycin fermentation, it was added to NTL

and NTH media at intervals of 5 mg/L final concentration (0–20 mg/L). At 120 h, the natamycin concentration in F607 was $\sim\!35.97\%$ higher in NTH medium supplemented with 5.0 mg/L NMN than in non-supplemented medium (Figure 3A). Under low organic carbon source conditions, the natamycin concentration was $\sim\!2.31$ -fold higher in F607 cells grown for 120 h in NTL medium containing 15 mg/L NMN than in cells grown in NTL medium alone (Figure 3B). Compared with NTL medium, the cells grown in NTH showed greater regeneration of intracellular NAD+ (Figure 3C), with a 1.87-fold (1.57 μ mol/g DCW) increase at 72 h.



Schematic overview of the links between metabolites and the expression profiles of genes involved in NAD⁺/NADP⁺ biosynthesis and natamycin production in *S. gilvosporeus* F607. Metabolite and gene expression levels represent the results of metabolomic and transcriptomic data from the rapid phase (60 h) of natamycin biosynthesis. Metabolites and genes shown in red were downregulated in high-nitrogen medium compared with that in low-nitrogen medium (NTH/NTL), those in green were upregulated (NTH/NTL), and those in black showed no difference. Numerical values represent log₂-fold changes of NTH60/NTL60.

These results confirmed that NMN supplementation could increase NAD⁺ concentrations, thereby improving natamycin biosynthesis.

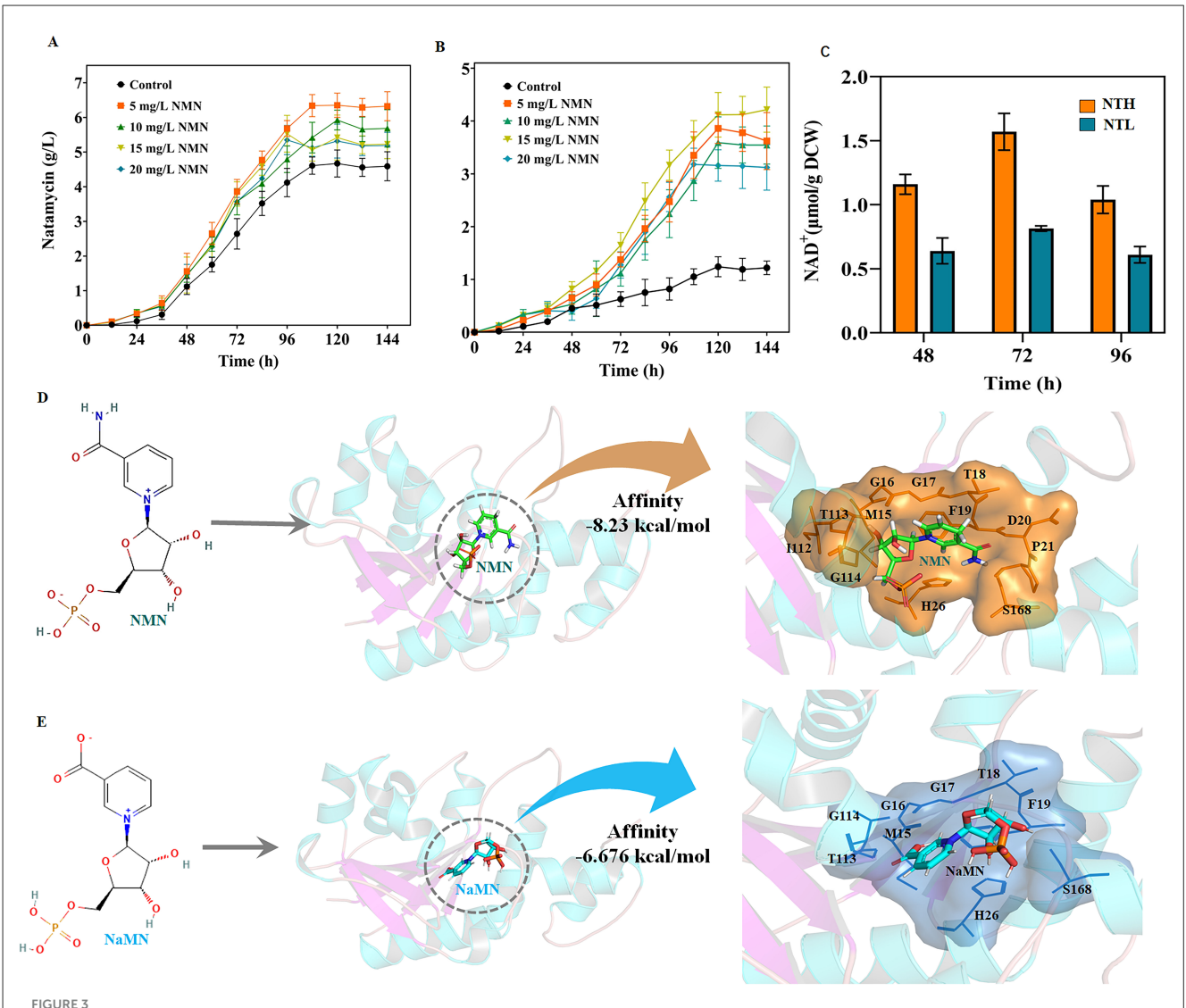
The NMN/NaMN adenylyltransferase encoded by *nadD*, collectively referred to as pyridine nucleotide adenylyltransferase, is an indispensable enzyme that catalyzes the central step of all NAD biosynthesis pathways, recognizing both NMN and NaMN as substrates (Zhang et al., 2003). Considering that the structural and catalytic properties of NadD have not been characterized in *S. gilvosporeus*, we examined the molecular features and substrate specificity of the novel enzyme NadDsg in strain F607. NadDsg was found to contain a central six-stranded parallel β-sheet flanked by eight helices in a typical Rossmann fold topology (Zhang et al., 2003) (Supplementary Figure 1). In *E. coli*, NadD strongly favors NaMN over NMN, catalyzing the formation of NAAD with 20-fold greater efficiency than NAD (Mehl et al., 2000; Wang et al., 2017). NadDsg showed only a slight preference for NMN (-8.23 kcal/mol affinity) over NaMN (-6.676 kcal/mol affinity) (Figures 3D, E).

In molecular simulation analysis, NadDsg was revealed to bind to NaMN through nine amino acid residues: Met15, Gly16, Gly17, Thr18, Phe19, His26, Thr113, Gly114, and Ser168 (Figure 3D). These residues are consistent with the conserved

GxFxPx[H/T]xxH and ISSTxxR motifs reported across humans, yeast, nematodes, and bacteria (Lau et al., 2009). Additionally, Asp20, Pro21, and Ile112 were predicted to contribute to substrate binding during NadDsg–NMN interaction (Figure 3E), while His26 forms stacking interactions with the pyridine ring and plays a critical role in NaMN recognition (Supplementary Figure 2). These findings suggested that, among the binding residues, Asp20, Pro21, and Ile112 may play major roles in substrate recognition by NadDsg.

3.4 NadDsg mutant constructions and screening with higher NMN preference

The above results indicate that NadDsg with higher NMN preference would be a convenient and fast way to enhance NAD⁺ and natamycin biosynthesis in F607 in the presence of NMN addition. To alter the substrate preference, we chose to make changes at 17 residues: Met15, Gly16, Gly17, Thr18, Phe19, His26, Thr113, Gly114, Ser168, Asp20, Pro21, Ile112, Tyr92,

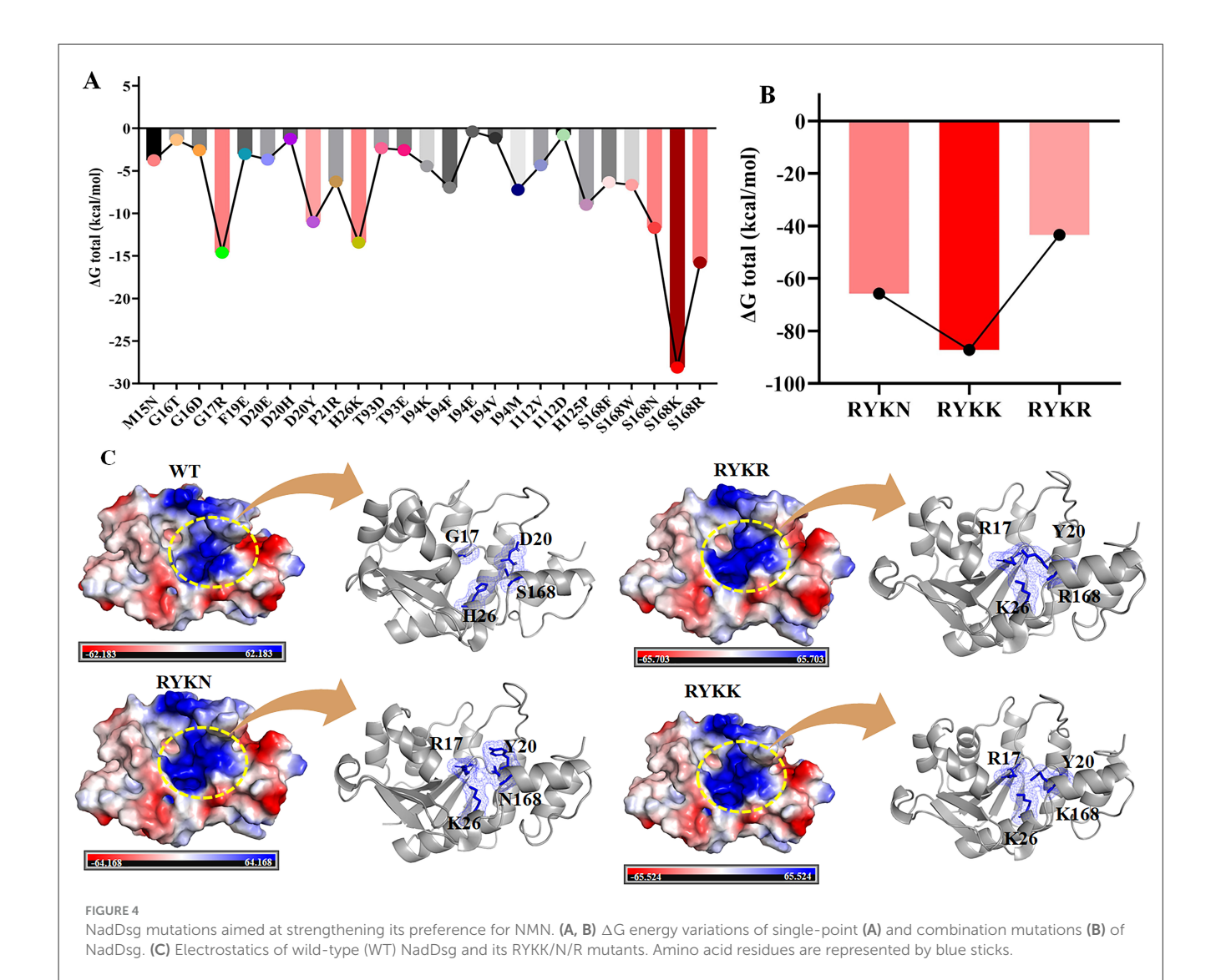


NMN supplementation promotes natamycin biosynthesis and NadDsg interactions with different substrates. (A, B) Natamycin production by S. gilvosporeus F607 cultivated under different levels of NMN supplementation in NTH (A) and NTL (B) media. (C) Concentrations of intracellular NAD⁺ in F607 cells cultivated in in NTH or NTL media. (D, E) Molecular simulations of NadDsg interactions with NMN (D) and NaMN (E). Substrate-binding sites are represented by color shadowing. Binding amino acid residues are represented by orange (NMN) and blue (NaMN) lines.

Thr93, Ile94, Trp124, and His125. Single-point virtual saturation mutagenesis of these amino acids yielded 338 virtual variants, among which 25 exhibited varying degrees of improved NMN binding ability (Figure 4A and Supplementary Table 4). Among the variants with significantly impacted binding ability, more than half (14) were located within the conserved GxFxPx[H/T]xxH and ISSTxxR motifs. Notably, the S168K mutant exhibited the most pronounce effect, with a total ΔG energy variation of -28.12 kcal/mol (Figure 4A). Additionally, the D20Y, S168N, H26K, G17R, and S168R mutants presented total ΔG energy variations of -11 kcal/mol, -11.69 kcal/mol, -13.43 kcal/mol, -14.61 kcal/mol, and -15.78 kcal/mol (Figure 4A), respectively, which were attributed to variations in van der Waals forces (ΔE_{vdw}) and electrostatic interaction (ΔE_{ele}) (Supplementary Table 4). These findings indicated a significant role of S168 in NadDsg-NMN binding.

Next we evaluated the combined effects of G17R, D20Y, and H26K with three S168 point mutations (S168R, S168K, and S168N), designated R¹⁷Y²⁰K²⁶R¹⁶⁸ (RYKR), R¹⁷Y²⁰K²⁶K¹⁶⁸ (RYKK), and R¹⁷Y²⁰K²⁶N¹⁶⁸ (RYKN), respectively. Among the S168 single variants, enzyme binding strength was ranked as S168K > S168R > S168N (Figure 4A). The total ΔG of the combined mutations RYKK and RYKN exceeded the sum of the corresponding single-point mutations, indicating synergistic effects. In contrast, the ΔG change of RYKR was less than the cumulative impact of its individual point mutations (Figure 4B and Supplementary Table 5). Overall, the binding strength of these combination mutants followed the order RYKK > RYKN > RYKR.

Kinetic analysis indicated that, compared with wild-type NadDsg, all three combination mutants had lower K_m values and higher k_{cat} values for NMN (Table 1). The catalytic efficiency (k_{cat}/K_m) of the mutants with respect to NMN was increased by



52.9-fold, 5.36-fold, and 9.36-fold, respectively, relative to NadDsg (Table 1). Additionally, the NadDsg_{RYKK} mutant exhibited an 55.26-fold increase in selectivity for NMN over NaMN (from 1.49 to 82.30) (Table 2), indicating a shift in substrate specificity and

enhanced preference for NMN.

Evaluation of the substrate-binding preferences of the combination mutants revealed that the RYKK/N/R mutations altered the binding pocket by inducing bending and extension (Figure 4C), leading to more stringent substrate selection and reduced accessibility. Compared to the NadDsg (wild type), NadDsgRYKK, NadDsgRYKN, and NadDsgRYKR changed the conformation of NMN binding cavity that composed by four amino acid residues (Supplementary Figure 3). In NadDsg, G17, D20, H26 and S168 composed a nearly cubic spatial structure (6.4Å \times 6.2Å \times 5.4Å \times 4.8Å). In mutants, all distances were shortened and led to a distorted structure, especially in NadDsgRYKK, elongated spatial structure (4.0Å \times 6.0Å \times 3.6Å \times 3.2Å) may cause an alternative bent and extended NMN conformations, which was reported to be a catalytic mechanism of NMN adenylyltransferase in Human (Zhang et al., 2003). Moreover, compared with wild-type NadDsg,

the mutations in NadDsgRYKK, NadDsgRYKN, and NadDsgRYKR all enhanced the electrostatics to different degrees (Figure 4C). Pyridine nucleotide adenylyltransferase has been proposed to use an in-line nucleophilic attack of the NMN phosphate on the ATP $\alpha\text{-phosphate}$ (Zhang et al., 2003). These enhanced electrostatics provided a more suitable chemical environment for nucleophilic attack and a stronger preference for NMN.

3.5 Supplementation of NMN and NadDsg_{RYKK} overexpression promotes natamycin biosynthesis

The integrated transcriptomic and metabolomic analyses suggested that NMN supplementation had a positive influence on natamycin biosynthesis in F607. To further increase natamycin production, a strain with overexpression of the NadDsgRYKK mutant (F607 $_{\rm RYKK}$) was constructed and cultivated in NTH medium supplemented with no NMN supplementation. At 120 h,

TABLE 1 Differential expression of natamycin biosynthesis PKS genes and NAD+/NADP+ biosynthesis genes.

Natamycin biosynthesis PKS genes			NAD ⁺ /NADP ⁺ biosynthesis genes			
Gene id	Gene Description	log2FoldChange (NTH/NTL)	id	Gene Description	log2FoldChange (NTH/NTL)	
B1H19_RS05020	SgnS4	5.698460908	B1H19_RS10955	NAD kinase	1.121823625	
B1H19_RS05025	SgnS3	5.126958996	B1H19_RS12720	NadA	2.201256121	
B1H19_RS05030	SgnS2	5.591874351	B1H19_RS14905	NadD	2.300976653	
B1H19_RS05075	SgnS0	6.106795442	B1H19_RS27920	NadE	2.577468633	
B1H19_RS05085	SgnS1	4.424676334	B1H19_RS29395	PncC	1.229274518	

TABLE 2 Kinetic parameters of wild-type and combination mutants of NadDsg.

Mutants of NadDsg	Kinetics for NMN			Kinetics for NaMN			Selectivity (k_{cat}/K_m)
	<i>K_m</i> (mM)	$k_{cat}(s^{-1})$	k_{cat}/K_m (mM $^{-1}$ s $^{-1}$)	<i>K_m</i> (mM)	$k_{cat}(s^{-1})$	k_{cat}/K_m (mM $^{-1}$ s $^{-1}$)	with NMN)/(k_{cat}/K_m with NaMN)
NadDsg	1.49	2.61	1.75	2.18	2.57	1.18	1.49
NadDsg _{RYKK}	0.11	12.12	110.18	3.72	4.98	1.34	82.30
NadDsg _{RYKN}	0.47	5.24	11.15	9.17	6.69	0.73	15.22
NadDsg _{RYKR}	0.34	6.17	18.15	5.31	16.26	3.06	5.93

natamycin production in strain F607_{RYKK} reached 5.24 g/L, compared with 4.67 g/L in strain F607, representing a 1.12-fold (p < 0.05) enhancement (Figure 5A).

Then, NMN was added to NTH medium at a final concentration of 5-15 mg/L. At 120 h, natamycin production by F607_{RYKK} reached 6.68 g/L in NTH medium supplemented with 10 mg/L NMN (increase by 0.275-fold, p < 0.05), compared with no NMN supplementation (5.24 g/L) (Figure 5B). Relative to F607 (4.67 g/L), NadDsgRYKK overexpression combined with 10 mg/L NMN supplementation led to a 43.1% increase (p < 0.05) increase in natamycin production (Figure 5B). Additionally, natamycin initiation occurred earlier (12-24 h) in the NadDsgRYKK overexpression strain, leading to increased demand for NMN. In the wild-type strain F607, 5 mg/L NMN represented the optimal supplementation level for natamycin biosynthesis (Figure 3A). In contrast, F607_{RYKK} required 10 mg/L NMN to reach its maximum natamycin production level, potentially reflecting differences in processing capacity between the native NadDsg and engineered NadDsgRYKK. These results indicated that NMN supplementation combined with NadDsg_{RYKK} overexpression is an effective strategy to enhance natamycin biosynthesis (Figure 5C). Gaining a deeper understanding of the functional roles of these motifs will inform future engineering strategies aimed at enhancing natamycin production.

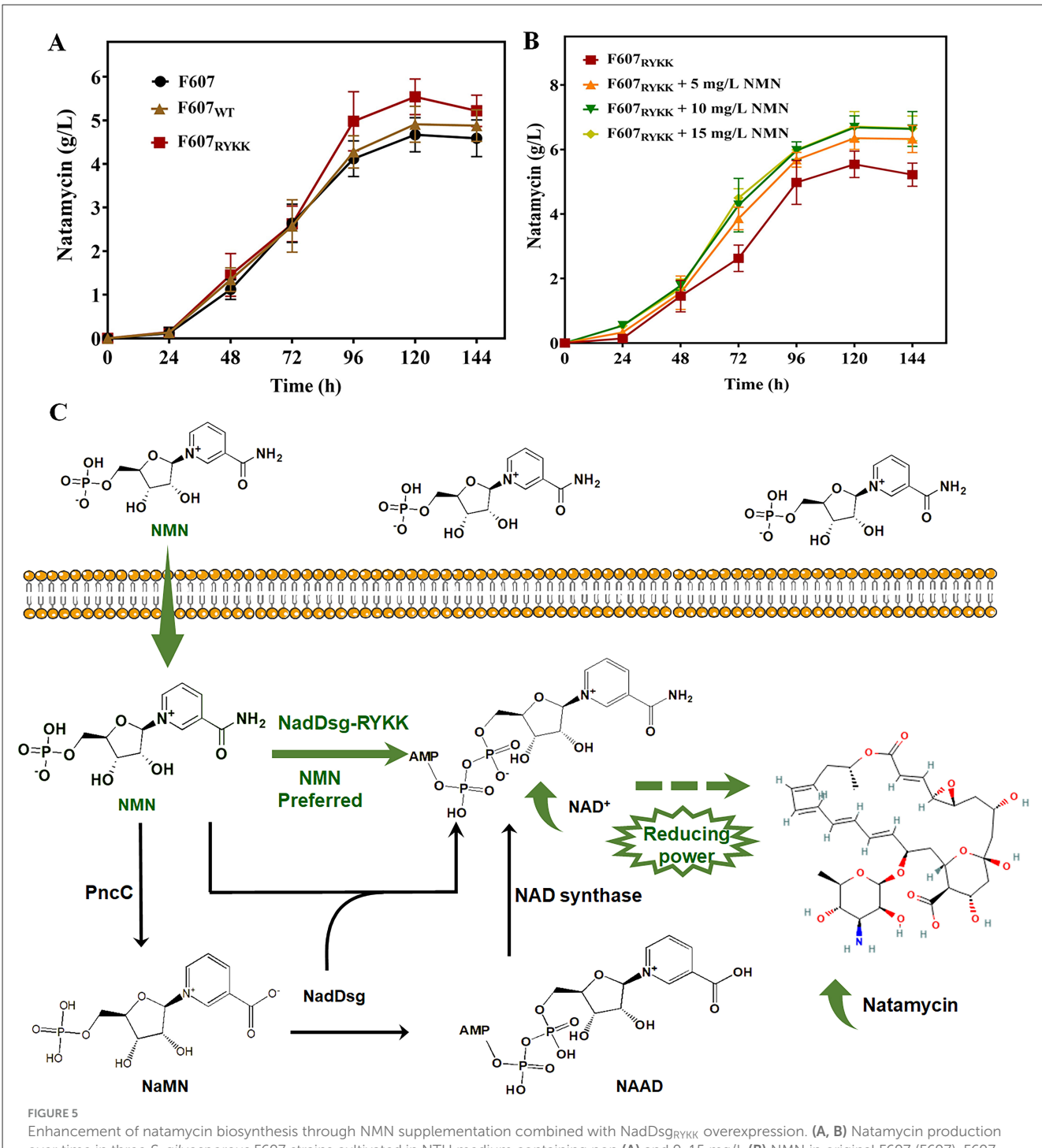
4 Discussion

Natamycin, a glycosylated 26-membered tetraene macrolide antifungal produced by multiple *Streptomyces* species, has become a major mold inhibitor in the food industry (Yangla and Yldz, 2016) and has shown potential for inhibiting cancer cell proliferation (Vasquez et al., 2020). Approaches to improve natamycin productivity have included optimization of large-scale

fermentation, classical random mutagenesis, genetic engineering (Aparicio et al., 2016), and introduction of chemical or biological elicitors (Zong et al., 2021). In addition to adequate amounts and types of carbon, nitrogen metabolism was confirmed as a key factor in the production of natamycin (Farid et al., 2000). Recently, overexpression of the nitrogen metabolism regulatory gene glnR in S. gilvosporeus was shown to increase natamycin production, achieving a final yield 1.67 times higher than that of the original strain (Wang et al., 2025b). In this study, our findings suggest that an abundance of organic nitrogen promotes natamycin production by enhancing the nicotinate/nicotinamide metabolic pathway, which may serve as a source of reducing power necessary for natamycin biosynthesis. Additionally, rapid biosynthesis of natamycin created high demand for NAD(H) and NADP(H). Accordingly, strategies that bolster reducing power may provide a viable means to increase natamycin yield.

For *Streptomyces*, amino acid metabolism and NAD synthesis are primary metabolism, which provide the precursors of secondary metabolism (Rodríguez et al., 2018). *S. gilvosporeus* F607 preferred the aspartic acid pathway rather than the tryptophan-Kynurenic acid pathway to synthesize NAD(P) in rich nitrogen. That may relate to the crosstalk between carbon, nitrogen regulation of secondary metabolism. It was reported that factors (such as ArgR and GlnR) linked the arginine and carbon metabolism (Rodríguez et al., 2018). In this study, we proposed that, to provide sufficient precursors for natamycin metabolism, *S. gilvosporeus* linked the metabolism of carbon and nitrogen through the Asp pathway (glutamic acid and oxaloacetic acid condensation) under high nitrogen source conditions.

Previously, 0.0025% (w/v) nicotinamide and 0.005% (w/v) NA, defined as growth promoters, were shown to enhance tacrolimus production in *S. tsukubaensis* by \sim 3-fold and \sim 6-fold, respectively, probably by stimulating NAD/NADP biosynthesis



Enhancement of natamycin biosynthesis through NMN supplementation combined with NadDsg_{RYKK} overexpression. (**A, B**) Natamycin production over time in three *S. gilvosporeus* F607 strains cultivated in NTH medium containing non (**A**) and 0-15 mg/L (**B**) NMN in original F607 (F607), F607 overexpressing wild-type NadDsg (F607_{WT}), and F607 overexpressing NadDsg_{RYKK} (F607_{RYKK}). (**C**) Schematic representation of the strategy used to enhance natamycin biosynthesis. Green represent the modified NMN preferred pathway of this study, black represent the original metabolic pathway.

(Turlo et al., 2012). Furthermore, upregulation of glycolysis and the PPP pathway increases the supply of pyruvate and NADPH, which are essential for the synthesis of acetyl-CoA and malonyl-CoA, as well as for providing reducing power during natamycin biosynthesis (Wang et al., 2025b). Here, integrated transcriptomic and metabolomic analyses of *S. gilvosporeus* F607 also revealed a link between natamycin biosynthesis and nicotinate/nicotinamide

metabolism, along with significant enhancement of the NAD biosynthesis pathway originating from Asp.

In *E. coli, de novo* NAD is synthesized via the deamidated or amidated pathways. In the deamidated pathways, NaMN is coupled with ATP by the action of NaMN adenylyltransferase to form NAAD, which is amidated to give NAD by the action of NAD synthetase encoded by *nadE* (D'Angelo et al., 2000). Alternatively,

in the amidated pathway, NAD can be synthesized via NMN adenylyltransferase catalysis, which directly converts NMN to NAD at the expense of ATP (Magni et al., 2009). However, the NMN adenylyltransferase in E. coli, NadD, strongly favors NaMN over NMN (Mehl et al., 2000). In S. gilvosporeus F607, we investigated the NAD biosynthetic pathway and the substrate preference of the NadD homolog NadDsg. NadDsg exhibited a slightly higher affinity for NMN (-8.23 kcal/mol) compared with NaMN (-6.676 kcal/mol), favoring a one-step catalytic path for NAD synthesis via the deamidated pathway. This preference may contribute to greater catalytic efficiency relative to the two-step amidated pathway. This metabolic paradox that S. gilvosporeus F607 does not carry a NAMPT enzyme to synthesize NMN but can use NMN by NadDsg to synthesize NAD may be related to two points. S. gilvosporeus is a soil microorganism, it need gain a competitive advantage by inhibit the growth of fungi or other bacteria (Evan et al., 2023). On the one hand, losing the ability to synthesize NMN during their evolution, may making their metabolism more efficient and rapid. On the other hand, transporting NMN from the soil environment is an economical and practical way for S. gilvosporeus form other NMN producing species, like plants, animals, or microorganisms (Shen et al., 2021). More investigations on the NMN transporter (encoded by B1H19_RS09230 gene in F607 genome) may be another effective strategy for enhancing the synthesis of natamycin.

Furthermore, the engineered mutant NadDsg_{RYKK} demonstrated an enhanced affinity for NMN. Given that most microbial cells lack the pathway required to synthesize NMN, NMN supplementation was applied to the NadDsg_{RYKK} overexpression strain F607_{RYKK} to boost natamycin production. At 120 h, the natamycin yield of F607_{RYKK} increase by a 43.1% increase, reached 6.68 g/L, compared with wild-type F607, confirming the efficacy of this strategy to enhance natamycin biosynthesis. Additionally, further researches on analysis of kinetic parameters of mutant enzymes and applicability of the production platform to other strains are needed.

5 Conclusion

This study elucidates a previously unrecognized regulatory mechanism linking organic nitrogen availability to natamycin biosynthesis in S. gilvosporeus F607 through NAD (P) cofactor elevation. Cultivation in organic nitrogen-rich medium enhanced NAD (P) pathway metabolites and established NAD(P) cofactor abundance as a critical mediator of nitrogen-driven secondary metabolism. The discovery and functional characterization of the NadDsg, which preferentially utilizes NMN over NaMN, provided a mechanistic target for metabolic engineering. Strategic supplementation with 10 mg/L NMN combined with overexpression of the engineered NadDsg_{RYKK} variant (with enhanced substrate specificity) synergistically boosted natamycin production to 6.68 g/L - a 43.1% improvement over the wild-type strain. The yield improvement through combined metabolic and enzyme engineering validates the translational potential of these findings for industrial-scale natamycin production.

Data availability statement

The original contributions presented in the study are included in the article/Supplementary material, further inquiries can be directed to the corresponding author.

Author contributions

ZM: Investigation, Writing – original draft. MY: Data curation, Formal analysis, Investigation, Writing – original draft. JW: Data curation, Methodology, Writing – original draft. HL: Investigation, Writing – original draft. WG: Investigation, Writing – original draft. PY: Investigation, Writing – original draft. XC: Investigation, Writing – original draft. JF: Validation, Visualization, Writing – original draft. GC: Formal analysis, Funding acquisition, Writing – review & editing. GZ: Conceptualization, Data curation, Formal analysis, Writing – review & editing.

Funding

The author(s) declare that financial support was received for the research and/or publication of this article. This work was supported by the Natural Science Foundation of Shandong Province [ZR2023MC068] and the National Natural Science Foundation of China [82204255].

Acknowledgments

We thank Jennifer Smith, PhD, and Michelle Kahmeyer-Gabbe, PhD, from Liwen Bianji (Edanz) (www.liwenbianji.cn) for editing the English text of a draft of this manuscript.

Conflict of interest

HL was employed by Shandong Freda Biotechnology Co., Ltd. The remaining authors declare that the research was conducted in the absence of any commercial or financial relationships that could be construed as a potential conflict of interest.

Generative AI statement

The author(s) declare that no Gen AI was used in the creation of this manuscript.

Any alternative text (alt text) provided alongside figures in this article has been generated by Frontiers with the support of artificial intelligence and reasonable efforts have been made to ensure accuracy, including review by the authors wherever possible. If you identify any issues, please contact us.

Publisher's note

All claims expressed in this article are solely those of the authors and do not necessarily represent those of

their affiliated organizations, or those of the publisher, the editors and the reviewers. Any product that may be evaluated in this article, or claim that may be made by its manufacturer, is not guaranteed or endorsed by the publisher.

Supplementary material

The Supplementary Material for this article can be found online at: https://www.frontiersin.org/articles/10.3389/fmicb.2025. 1684019/full#supplementary-material

References

- Antón, N., Mendes, M. V., Martin, J., f., and Aparicio, J. F. (2004). Identification of PimR as a positive regulator of pimaricin biosynthesis in *Streptomyces natalensis. J. Bacteriol.* 186, 2567–2575. doi: 10.1128/JB.186.9.2567-2575.2004
- Aparicio, J. F., Barreales, E. G., Pedro, A. D., Payero, T. D., and Santos-Aberturas, J. (2016). Biotechnological production and application of the antibiotic pimaricin: biosynthesis and its regulation. *Appl. Microbiol. Biotechnol.* 100, 61–78. doi: 10.1007/s00253-015-7077-0
- Aparicio, J. F., Caffrey, P., Gil, J. A., and Zotchev, S. B. (2003). Polyene antibiotic biosynthesis gene clusters. *Appl. Microbiol. Biotechnol.* 61, 179–188. doi: 10.1007/s00253-002-1183-5
- Aparicio, J. F., Fouces, R., Mendes, M. V., Olivera, N., and Martin, J. F. (2000). A complex multienzyme system encoded by five polyketide synthase genes is involved in the biosynthesis of the 26-membered polyene macrolide pimaricin in *Streptomyces natalensis*. *Chem. Biol.* 7, 895–905. doi: 10.1016/S1074-5521(00)00038-7
- BIOVIA. (2017). Discovery Studio Modeling Environment, Release 2017. San Diego, CA: Dassault Systèmes.
- Borgos, S. E. F., Sletta, H., Fjærvik, E., Brautaset, T., Ellingsen, T. E., Gulliksen, O.-M., et al. (2006). Effect of glucose limitation and specific mutations in the module 5 enoyl reductase domains in the nystatin and amphotericin polyketide synthases on polyene macrolide biosynthesis. *Arch. Microbiol.* 185, 165–171. doi: 10.1007/s00203-005-0083-3
- Butler, M. J., Bruheim, P., Jovetic, S., Marinelli, F., Postma, P. W., and Bibb, M. J. (2002). Engineering of primary carbon metabolism for improved antibiotic production in *Streptomyces lividans*. *Appl. Environ. Microbiol.* 68, 4731–4739. doi: 10.1128/AEM.68.10.4731-4739.2002
- D'Angelo, I., Raffaelli, N., Dabusti, V., Lorenzi, T., Magni, G., and Rizzi, M. (2000). Structure of nicotinamide mononucleotide adenylyltransferase: a key enzyme in NAD(+) biosynthesis. Structure~8,993-1004.~doi:~10.1016/S0969-2126(00)00190-8
- Ding, Y., Li, X., Horsman, G. P., Li, P., Wang, M., Li, J., et al. (2021). Construction of an alternative NAD $^+$ de novo biosynthesis pathway. *Adv. Sci.* 8:202004632. doi: 10.1002/advs.202004632
- Du, Y. L., Chen, S. F., Cheng, L. Y., Shen, X. L., Tian, Y., and Li, Y. Q. (2009). Identification of a novel *Streptomyces chattanoogensis* L10 and enhancing its natamycin production by overexpressing positive regulator ScnRII. *J. Microbiol.* 47, 506–513. doi: 10.1007/s12275-009-0014-0
- Evan, M. F. S., Christine, R. B., and Marie, A. E. (2023). Streptomyces behavior and competition in the natural environment. *Curr. Opin. Microbiol.* 71:102257. doi:10.1016/j.mib.2022.102257
- Farid, M., Enshasy, H. E., El-diwany, A. I., and Elsayed, E. A. (2020). Optimization of the cultivation medium for natamycin production by *Streptomyces natalensis*. *J. Basic Microbiol.* 40, 333–342. doi: 10.1002/1521-4028(200012)
- Farid, M. A., el-Enshasy, H. A., el-Diwany, A. I., and el-Sayed el, S. A. (2000). Optimization of the cultivation medium for natamycin production by *Streptomyces natalensis. J. Basic Microbiol.* 40, 157–166. doi: 10.1002/1521-4028(200007)40:3andlt;157::AID-
- Fink, D., Weißschuh, N., Reuther, J., Wohlleben, W., and Engels, A. (2002). Two transcriptional regulators GlnR and GlnRII are involved in regulation of nitrogen metabolism in *Streptomyces coelicolor* A3(2). *Mol. Microbiol.* 46, 331–347. doi: 10.1046/j.1365-2958.2002.03150.x
- Fu, J., Qin, R., Zong, G., Liu, C., Kang, N., Zhong, C., et al. (2019). The CagRS two-component system regulates clavulanic acid metabolism via multiple pathways in *Streptomyces clavuligerus* F613-1. *Front. Microbiol.* 10:244. doi: 10.3389/fmicb.2019.00244
- Gongli, Z., Guangxiang, C., Jiafang, F., Peipei, Z., Xi, C., Wenxiu, Y., et al. (2022). MacRS controls morphological differentiation and natamycin biosynthesis in *Streptomyces gilvosporeus* F607. *Microbiol. Res.* 262:127077. doi: 10.1016/j.micres.2022.127077
- Krysenko, S., and Wohlleben, W. (2024). Role of carbon, nitrogen, phosphate and sulfur metabolism in secondary metabolism precursor supply in *Streptomyces* spp. *Microorganisms* 12:1571. doi: 10.3390/microorganisms12081571

- Lau, C., Niere, M., and Ziegler, M. (2009). The NMN/NaMN adenylyltransferase (NMNAT) protein family. FBL 14, 410–431. doi: 10.2741/3252
- Liang, J. L., Xu, Z., Liu, T., Lin, J., and Cen, P. (2008). Effects of cultivation conditions on the production of natamycin with *Streptomyces gilvosporeus* LK-196. *Enzyme Microb. Technol.* 42, 145–150. doi: 10.1016/j.enzmictec.2007.08.012
- Madeira, F., Park, Y. M., Buso, J. L. N., Gur, T., Madhusoodanan, N., et al. (2019). The EMBL-EBI search and sequence analysis tools APIs in 2019. *Nucleic Acids Res.* 47, 636–641. doi: 10.1093/nar/gkz268
- Magni, G., Di Stefano, M., Orsomando, G., Raffaelli, N., and Ruggieri, S. (2009). NAD(P) biosynthesis enzymes as potential targets for selective drug design. *Curr. Med. Chem.* 16, 1372–1390. doi: 10.2174/092986709787846505
- Martín, J. F., and Liras, P. (2010). Engineering of regulatory cascades and networks controlling antibiotic biosynthesis in Streptomyces. *Curr. Opin. Microbiol.* 13, 263–273. doi: 10.1016/j.mib.2010.02.008
- Mehl, R. A., Kinsland, C., and Begley, T. P. (2000). Identification of the *Escherichia coli* nicotinic acid mononucleotide adenylyltransferase gene. *J. Bacteriol. Parasitol.* 182, 4372–4374. doi: 10.1128/JB.182.15.4372-4374.2000
- Passmore, M., Gallo, A., Lewandowski, J. R., and Jenner, M. (2021). Molecular basis for acyl carrier protein–ketoreductase interaction in trans-acyltransferase polyketide synthases. *Chem. Sci.* 12, 13676–13685. doi: 10.1039/D1SC03478B
- Rodríguez, A. R., Carmona, N. M., Villafán, B. R., Koirala, N., Rocha, D., and Sánchez, S. (2018). Interplay between carbon, nitrogen and phosphate utilization in the control of secondary metabolite production in *Streptomyces*. *Antonie Van Leeuwenhoek* 111, 761–781. doi: 10.1007/s10482-018-1073-1
- Ryu, Y. G., Butler, M. J., Chater, K. F., and Lee, K. J. (2006). Engineering of primary carbohydrate metabolism for increased production of actinorhodin in *Streptomyces coelicolor*. *Appl. Environ. Microbiol.* 72, 7132–7139. doi: 10.1128/AEM.01308-06
- Shen, Q., Zhang, S. J., Xue, Y. Z., Peng, F., Cheng, D. Y., Xue, Y. P., et al. (2021). Biological synthesis of nicotinamide mononucleotide. *Biotechnol. Lett.* 43, 2199–2208. doi: 10.1007/s10529-021-03191-1
- Turło, J., Gajzlerska, W., Klimaszewska, M., Król, M., Dawidowski, M., and Gutkowska, B. (2012). Enhancement of tacrolimus productivity in *Streptomyces tsukubaensis* by the use of novel precursors for biosynthesis. *Enzyme Microb. Technol.* 51, 388–395. doi: 10.1016/j.enzmictec.2012.08.008
- Vasquez, J. L., Lai, Y., Annamalai, T., Jiang, Z., Zhang, M., Lei, R., et al. (2020). Inhibition of base excision repair by natamycin suppresses prostate cancer cell proliferation. *Biochimie* 168, 241–250. doi: 10.1016/j.biochi.2019.11.008
- Volpon, L., and Lancelin, J. M. (2002). Solution NMR structure of five representative glycosylated polyene macrolide antibiotics with a steroldependent antifungal activity. $Eur.\ J.\ Biochem.\ 269,\ 4533-4541.\ doi:\ 10.1046/j.1432-1033.2002.03147.x$
- Wang, L., Xiao, W., Qiu, T., Zhang, H., Zhang, J., and Chen, X. (2025a). Enhanced Natamycin production in *Streptomyces gilvosporeus* through phosphate tolerance screening and transcriptome-based analysis of high-yielding mechanisms. *Microb. Cell Fact.* 24:79. doi: 10.1186/s12934-025-02696-y
- Wang, L., Xiao, W., Zhang, H., Zhang, J., and Chen, X. (2025b). Improved natamycin production in *Streptomyces gilvosporeus* through mutagenesis and enhanced nitrogen metabolism. *Microorganisms* 13:13020390. doi: 10.3390/microorganisms13020390
- Wang, M., Wang, S., Zong, G., Hou, Z., Liu, F., Liao, D. J., et al. (2016). Improvement of natamycin production by cholesterol oxidase overexpression in *Streptomyces gilvosporeus*. *J. Microbiol. Biotechnol.* 26, 241–247. doi: 10.4014/jmb.1505.05033
- Wang, X., Zhou, Y. J., Wang, L., Liu, W., Liu, Y., Peng, C., et al. (2017). Engineering *Escherichia coli* nicotinic acid mononucleotide adenylyltransferase for fully active amidated nad biosynthesis. *Appl. Environ. Microbiol.* 83, e00692-17. doi: 10.1128/AEM.00692-17
- Wu, Q., Bai, L., Liu, W., Li, Y., Lu, C., Li, Y., et al. (2013). Construction of a *Streptomyces lydicus* A01 transformant with a chit42 gene from *Trichoderma harzianum* P1 and evaluation of its biocontrol activity against *Botrytis cinerea*. *J. Microbiol.* 51, 166–173. doi: 10.1007/s12275-013-2321-8

Xavier, R., and Patrice, G. (2014). Deciphering key features in protein structures with the new ENDscript server. *Nucleic Acids Res.* 42, 320–324. doi:10.1093/nar/gku316

Xianzhong, C., Mingming, L., Li, Z., Wei, S., Govender, A., You, F., et al. (2014). Metabolic engineering of *Escherichia coli* for improving shikimate synthesis from glucose. *Bioresour. Technol.* 166, 64–71. doi: 10.1016/j.biortech.2014. 05.035

Yangla, F., and Yldz, P. O. (2016). Casein/natamycin edible films efficiency for controlling mould growth and on microbiological, chemical and sensory properties during the ripening of Kashar cheese. *J. Sci. Food Agric.* 96, 2328–2336. doi: 10.1002/jsfa.7348

Zhang, B., Zhang, Y.-H., Chen, Y., Chen, K., Jiang, S.-X., Huang, K., et al. (2020). Enhanced AmB production in *Streptomyces nodosus* by fermentation

regulation and rational combined feeding strategy. Front. Bioeng. Biotechnol. 8:00597. doi: 10.3389/fbioe.2020.00597

Zhang, X., Kurnasov, O. V., Karthikeyan, S., Grishin, N. V., Osterman, A. L., and Zhang, H. (2003). Structural characterization of a human cytosolic NMN/NaMN adenylyltransferase and implication in human NAD biosynthesis. *J. Biol. Chem.* 278, 13503–13511. doi: 10.1074/jbc.M300073200

Zhang, Y., Huang, Z., Du, C., Li, Y., and Cao, Z., a. (2009). Introduction of an NADH regeneration system into *Klebsiella oxytoca* leads to an enhanced oxidative and reductive metabolism of glycerol. *Metab. Eng.* 11, 101–106. doi: 10.1016/j.ymben.2008.11.001

Zong, G. L., Fu, J., Zhang, P., Zhang, W., Xu, Y., Cao, G., et al. (2021). Use of Elicitors to Enhance or Activate the Antibiotic Production in Streptomyces. Crit. Rev. Biotechnol. 42, 1260–1283. doi: 10.1080/07388551.2021.1987856